

Assessment of Ventricular Septal Defect Size and Morphology by Three-Dimensional Transthoracic Echocardiography

Khaled Hadeed, MD, Sébastien Hascoet, MD, Romain Amadiou, MD, Clément Karsenty, MD, Fabio Cuttone, MD, Bertrand Leobon, MD, PhD, Yves Dulac, MD, and Philippe Acar, MD, PhD,
Toulouse, France

Background: Morphologic description of ventricular septal defect (VSD) is mandatory before performing the newly developed transcatheter closure procedure. Inaccurate estimation of defect size has been reported using conventional two-dimensional (2D) transthoracic echocardiography (TTE). The aim of this study was to assess VSD morphology and size using three-dimensional (3D) TTE compared with 2D TTE and surgery.

Methods: Forty-eight children aged 21.4 ± 29.3 months with isolated muscular ($n = 11$ [22.9%]) and membranous ($n = 37$ [77.1%]) VSDs were prospectively included. Three-dimensional images were acquired using full-volume single-beat mode. Minimal diameter, maximal diameter, and systolic and diastolic VSD areas were measured from 3D data sets using multiplanar reconstruction mode (QLAB 9). Maximal-to-minimal VSD diameter ratio was used to assess VSD geometry. Linear regression analysis and the Bland-Altman method were used to compare 3D measurements with 2D and surgical measurements in a subgroup of 15 patients who underwent surgical VSD closure.

Results: VSD 3D diameters and areas were measured in all patients (100%; 95% CI, 92.6%-100%). Maximal diameter was lower on 2D TTE compared with 3D TTE (7.3 vs 11.3 mm, $P < .0001$). Mean bias was 4 mm, with 95% of values ranging from -1.76 to 9.75 mm. Correlation between 3D maximal diameter and surgical diameter was strong ($r^2 = 0.97$, $P < .0001$), while correlation between maximal 2D diameter and surgical diameter was moderate ($r^2 = 0.63$, $P < .0001$). VSDs had an oval shape when assessed by 3D TTE. Maximal-to-minimal diameter ratio assessed by 3D TTE was significantly higher in muscular VSDs compared with membranous VSDs (3.20 ± 1.51 vs 2.13 ± 1.28 , respectively, $P = .01$). VSD area variation throughout the cardiac cycle was 32% and was higher in muscular compared with membranous VSDs (49% vs 26%, $P = .0001$).

Conclusions: Three-dimensional TTE allows better VSD morphologic and maximal diameter assessment compared with 2D TTE. VSD shape and its changes during the cardiac cycle can be visually and quantitatively displayed. Three-dimensional echocardiography may thus be particularly useful before and during percutaneous VSD closure. (J Am Soc Echocardiogr 2016; ■: ■-■.)

Keywords: Ventricular septal defect, Three-dimensional echocardiography, Children

Indications for surgical closure of congenital ventricular septal defects (VSDs) are based on pulmonary pressure and left ventricular volume overload.¹ Two-dimensional (2D) transthoracic echocardiography (TTE) is usually sufficient to assess the anatomy and hemodynamics of a VSD and guide clinical management.^{1,2} Recently, percutaneous

From the Pediatric Cardiology Unit (K.H., S.H., R.A., C.K., Y.D., P.A.) and the Cardiac Surgery Unit (F.C., B.L.), Children Hospital, CHU, Toulouse, France; and Inserm UMR1048, Institut des Maladies Métaboliques et Cardiovasculaires, Toulouse, F-31000, France (C.K., S.H.).

Reprint requests: Khaled Hadeed, MD, Pediatric Cardiology, Children's Hospital, 330 Avenue de Grande Bretagne, TSA 70034, 31059 Toulouse Cedex 9, France (E-mail: hadeed.k@chu-toulouse.fr).

0894-7317/\$36.00

Copyright 2016 by the American Society of Echocardiography.

<http://dx.doi.org/10.1016/j.echo.2016.04.012>

closure of muscular as well as membranous VSDs using different devices has emerged as an alternative to the surgical technique in selected cases.³⁻⁶ An accurate assessment of the size and morphology of a VSD is of crucial importance in these cases for device choice. Morphologic assessment of VSD, its diameters, and its dynamic variation throughout the cardiac cycle are difficult to achieve from sequential cuts of one plane by 2D TTE.^{4,7-10} We and others have reported that three-dimensional (3D) TTE is useful to describe the size, morphology, and dynamic morphology variation of intracardiac defects such as atrial septal defects in children.^{11,12} Thus, we hypothesized that 3D TTE would also be useful to assess VSD morphology and size in these population. Our aim was to compare the 3D measurement of VSDs with that by 2D TTE and with surgical findings in a pediatric population. We also aimed to describe and compare the shapes of membranous and muscular VSDs throughout the cardiac cycle using 3D TTE.

Abbreviations**3D** = Three-dimensional**TTE** = Transthoracic echocardiography**2D** = Two-dimensional**VSD** = Ventricular septal defect**METHODS****Study Design**

We performed a prospective single-center study including 48 unselected children with isolated membranous or muscular VSDs. Patients with multiple VSDs and patients with other congenital cardiovascular abnormalities were

not included. The study was approved by our institutional review committee, and informed consent was obtained from each patient or his or her legal representative.

Echocardiographic Assessment

Two-dimensional TTE was used first to assess VSD size. Measurements were obtained from two orthogonal planes (long- and short-axis views) on the end-diastolic frames. The largest diameter of these two orthogonal diameters was considered the maximal 2D diameter and the smallest the minimal 2D diameter. A 3D full-volume single-beat data set was then acquired (iE33; Philips Medical Systems, Andover, MA) using X5-1 or X7-2 matrix probes (Philips Medical Systems). The data set was stored digitally and transferred to a workstation (QLAB 9; Philips Medical Systems) for offline analysis. All measurements from 3D data sets were independently performed by another operator, who was unaware of the results of 2D TTE.

The 3D data set analysis was performed using multiplanar reconstruction mode. Each of the three axes was moved to obtain a plane along the ventricular septum including the whole VSD from the en face view (Figure 1, Video 1; available at www.onlinejase.com). The two orthogonal diameters of the VSD were measured from this view on the end-diastolic frames. The largest diameter was considered the maximal 3D diameter and the smallest the minimal 3D diameter. The ratio of maximal to minimal 2D and 3D VSD diameters was calculated. Systolic and diastolic VSD areas were also obtained by delineating the outline of the VSD on the end-systolic and end-diastolic frames, respectively. The variation of the VSD surface area throughout the cardiac cycle was calculated as (diastolic VSD area – systolic VSD area)/diastolic VSD area and expressed as a percentage. All measurements were obtained from the right-sided surface of the VSD.

Surgical Measurements

In 15 children (31.3%; 95% CI, 18.7%-46.3%) who underwent surgical VSD closure, the defect was examined by the surgeon from the right ventricular side through a standard right atrial opening. The maximal diameter of the VSD was measured directly by the surgeon.

Statistical Analysis

Quantitative variables are expressed as mean \pm SD. Body surface area was calculated according to the Mosteller formula. Comparisons between measurements were performed using paired *t* tests or Wilcoxon signed rank test. Paired *t* tests were used when variables were normally distributed and after the homogeneity of variance was checked. The Shapiro-Wilk test was used to test the normality of distribution. The Levene test was used to assess the homogeneity of variance. When these conditions were not satisfied,

a nonparametric Wilcoxon test was used. Correlations between normally distributed variables were assessed using the Pearson test. Otherwise, a Spearman correlation coefficient was estimated.

A linear regression plot analysis expressing 3D diameters according to 2D diameters was performed for the whole population and among subgroups according to the position of the defect. The same method was applied to display 2D and 3D diameters according to surgical findings. The Bland-Altman method was used to further explore agreement between the two techniques.¹³ *P* values < .05 were considered to indicate statistical significant. Statistical analysis was performed using Stata version 8 (StataCorp LP, College Station, TX).

RESULTS**Study Population**

Forty-eight patients with isolated VSDs were included. VSDs were membranous in 37 patients (77.1%) and muscular in 11 (22.9%). Surgical VSD closure was performed in 15 patients (31.3%). Characteristics of the whole study population and of subgroups according to the position of the defect are reported in Table 1. The mean age of the study population was 21.4 \pm 29.3 months (range, 1-123 months). There was a trend toward younger children in the muscular VSD group.

VSD Measurements on 2D and 3D TTE

Acquisition of a 3D volume data set and measurements were feasible in all children (100%; 95% CI, 92.6%-100%). The mean obtained 3D image resolution was 30 MHz (range, 22-35 MHz).

VSD measurements using 2D and 3D TTE in the whole study population and among subgroups according to the position of the defect are reported in Table 2. Maximal and minimal VSD diameters were not significantly different between the two subgroups.

Correlation between maximal 3D and 2D diameters was moderate (Spearman correlation coefficient = 0.51, *P* < .001). Correlation between minimal 3D and 2D diameters was good (Spearman correlation coefficient = 0.75, *P* < .0001). Linear regression plots expressing 3D diameters according to 2D diameters are displayed in Figure 2 for the whole population and among subgroups according to the position of the defect. Minimal 3D and 2D diameters were well correlated ($r^2 = 0.77$, *P* < .0001). Correlation between 3D and 2D maximal diameters was significant, but the strength of the correlation was low ($r^2 = 0.29$, *P* < .0001). Correlation between 3D and 2D maximal diameters was better in membranous versus muscular VSDs ($r^2 = 0.46$ vs $r^2 = 0.11$). Correlations between 3D and 2D minimal diameters remained very good in membranous and muscular VSDs ($r^2 = 0.72$ and $r^2 = 0.90$).

Maximal diameter assessed by 2D TTE was lower than by 3D TTE (*P* < .0001). Bland-Altman analysis confirmed a mean bias of 4 mm. The magnitude of intertechnique differences observed for individual patients was quite high; 95% of values ranged from –1.76 to 9.75 mm. Mean bias was higher in muscular compared with membranous VSDs (6.02 vs 3.39 mm, respectively) (Figure 3).

Although VSD minimal diameter was significantly lower by 2D TTE compared with 3D TTE (*P* = .001), the difference was less pronounced. Mean bias was low, with a mean difference of 0.44 mm (Figure 3). The magnitude of intertechnique differences observed for individual patients was quite low; 95% of values ranged from –1.80 to 2.69 mm. Trends were similar with regard to membranous and muscular subgroups.

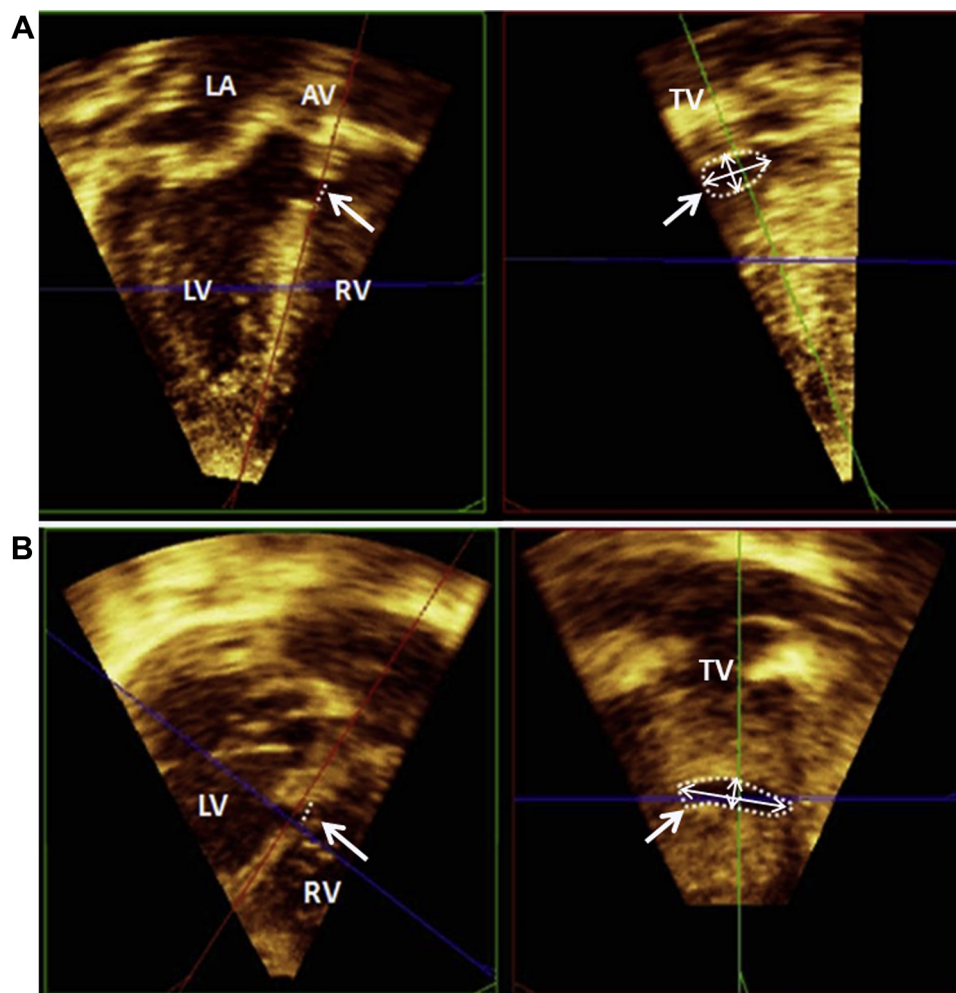


Figure 1 Multiplanar reconstruction (MPR) analysis. Diameters and areas of membranous (**A**) and muscular (**B**) VSDs (arrows) using MPR mode. The red axis was positioned along the interventricular septum to obtain a red plane including the whole VSD. Minimal and maximal VSD diameters were measured on this plane, and VSD area was delineated. AV, Aortic valve; LA, left atrium; LV, left ventricle; RV, right ventricle; TV, tricuspid valve.

Table 1 Characteristics of the study population

	All (n = 48)	Muscular VSD (n = 11 [22.9%])	Membranous VSD (n = 37 [77.1%])	P
Age (mo)	21.4 ± 29.3	10.4 ± 18.9	24.7 ± 31.3	.06
Weight (kg)	9.3 ± 7.3	6.8 ± 4.8	10.0 ± 7.8	.07
Height (cm)	74.3 ± 24.1	65.0 ± 18.8	77.1 ± 25.0	.10
BSA (m ²)	0.4 ± 0.2	0.3 ± 0.2	0.4 ± 0.2	.07
Surgical VSD closure	n = 15 (31.3%)	n = 4 (36.4%)	n = 10 (27.0%)	

BSA, Body surface area.

Data are expressed as mean ± SD or as number (percentage).

VSD Measurements by Echocardiography Compared with Surgical Findings

VSD maximal diameters obtained by 2D and 3D TTE in 15 patients who underwent surgical repair were compared with surgical findings (summarized in Table 3). Surgical and 3D diameters were not signif-

icantly different from and higher than 2D diameters. Correlation between maximal 3D and surgical diameters was excellent (Spearman correlation coefficient = 0.98, $P < .0001$). Correlation between maximal 2D and surgical diameters was good (Spearman correlation coefficient = 0.73, $P < .01$). Linear regression analysis of surgical diameter measurements confirmed an excellent correlation with maximal 3D diameter ($r^2 = 0.97$, $P < .0001$). Bland-Altman analysis confirmed the lack of any significant bias. The mean difference between surgical and 3D measurements was 0.25 mm, with 95% of values ranging from 1.35 to 0.85 mm. The correlation between surgical diameter and 2D maximal diameter was lower ($r^2 = 0.63$, $P < .0001$). The mean maximal 2D diameter was significantly lower than mean surgical measurements ($P < .001$). The mean bias by Bland-Altman analysis was 3.71 mm, with 95% of values ranging from -7.85 to 0.43 mm (Figure 4).

VSD Morphology

Maximal-to-minimal VSD diameter ratio was used to assess VSD geometry. Therefore, a ratio of 1 represents a perfect circle, while a progressively higher ratio represents a more elliptical geometry.

Table 2 VSD measurements by 2D and 3D TTE in the whole study population and in subgroups according to defect position

	All (n = 48)	Muscular VSD (n = 11)	Membranous VSD (n = 37)	P
2D TTE				
Maximal diameter (mm)	7.3 ± 2.4	6.0 ± 2.5	7.7 ± 2.3	.06
Minimal diameter (mm)	5.1 ± 2.0	4.2 ± 2.2	5.4 ± 1.9	.05
Maximal-to-minimal diameter ratio	1.5 ± 0.4	1.5 ± 0.3	1.5 ± 0.5	.48
3D TTE				
Maximal diameter (mm)	11.3 ± 3.3	12.1 ± 3.0	11.1 ± 3.4	.20
Minimal diameter (mm)	5.6 ± 2.2	4.5 ± 2.1	5.9 ± 2.1	.07
Maximal-to-minimal diameter ratio	2.3 ± 1.4	3.2 ± 1.5	2.1 ± 1.3	.01
dVSDA (cm ²)	0.6 ± 0.3	0.5 ± 0.4	0.6 ± 0.3	.51
sVSDA (cm ²)	0.4 ± 0.3	0.3 ± 0.2	0.4 ± 0.3	.05
Surface area variation (%)	32 ± 15	49 ± 11	26 ± 12	<.001

dVSDA, Diastolic VSD area; sVSDA, systolic VSD area.
Data are expressed as mean ± SD.

VSDs had an oval shape when assessed by 3D TTE. The mean maximal-to-minimal diameter ratio was higher by 3D TTE than 2D TTE. Maximal-to-minimal diameter ratio assessed by 3D TTE was significantly higher in muscular VSDs compared with membranous VSDs (3.20 ± 1.51 vs 2.13 ± 1.28 , respectively, $P = .01$) (Figure 5).

VSD Measurement Variation during the Cardiac Cycle

Diastolic VSD area was higher than systolic VSD area (0.6 ± 0.3 vs 0.4 ± 0.3 mm, $P < .0001$). VSD area variation during the cardiac cycle was $32 \pm 15\%$. It was significantly higher in muscular compared with membranous VSDs ($49 \pm 11\%$ vs $26 \pm 12\%$, $P < .001$). Figure 6 displays 3D en face views of membranous (Figure 6A) and muscular (Figure 6B) VSDs in systole and diastole illustrating variation throughout the cardiac cycle (Videos 2 and 3; available at www.onlinejase.com).

Interobserver Variability

Three-dimensional transthoracic echocardiographic measurements of VSDs performed by two blinded observers did not differ significantly. The coefficients of variation for interobserver variability were 3% (95% CI, 1.4%-4.6%) for maximal 3D diameter and 5.5% (95% CI, 2.5%-8.5%) for VSD area.

DISCUSSION

Our study illustrates some advantages of 3D TTE and some limitations of 2D TTE in the assessment of VSD shape and size in children. Assessment of VSDs is usually done using 2D TTE, which often provides enough information for patient management.¹⁴ However 2D TTE lacks the ability to display the entire shape of a defect in a single plane. Two-dimensional measurements are usually made in two orthogonal planes to assess VSD morphology. The maximal length and breadth of a defect are not easily obtained in standard views. Moreover, accurate sizing by 2D TTE using a single plane is even more difficult given the dynamic changes in VSD size in a beating heart during the cardiac cycle. High feasibility and

accuracy of 3D TTE to assess VSDs have been recently reported and confirmed in our work.¹⁵ In this study, we used a single-beat 3D acquisition to avoid stitching artifacts secondary to respiration, probe translation, and heart motion variation, which are difficult to avoid in young children. Image quality and resolution were acceptable to analyze VSDs. The shape of a VSD and its dynamic motion throughout the cardiac cycle can be displayed using 3D-unique en face views.¹⁶⁻¹⁸ In our study, measurements of VSD dimensions by echo-cardiography were performed from the right ventricular side to be in agreement with surgical measurements. Surgical sizing was performed on an empty, flaccid heart which usually has been arrested by cardioplegia after the institution of bypass. However, we found a close correspondence between maximal diameter obtained by 3D TTE and maximal surgical diameter. This confirms the high accuracy of 3D TTE for VSD sizing. On the other hand, we observed that 2D TTE underestimates maximal defect size compared with 3D TTE and surgical findings. This observation may be because the 2D transthoracic echocardiographic method is based on the short-axis plane, in which the ultrasound beams may not be perfectly parallel to the maximal axis of the defect. This limitation had greater impact when the defect was more oval shaped, with a higher maximal-to-minimal diameter ratio, as in muscular defects. Our study is the first to compare both minimal and maximal diameters between 2D and 3D TTE. Chen *et al.*¹⁹ reported a good correlation between VSD diameters obtained by 2D and 3D TTE with surgical findings. However, they only used the diameter derived from the four-chamber view by 2D TTE, which corresponds to the minimal diameter in our study. Van den Bosch *et al.*²⁰ used only maximal 2D diameter compared with 3D TTE and surgical findings. They showed that there was a weak correlation between maximal 2D and 3D diameters and between maximal 2D and surgical findings. Our results unify these discrepancies, confirming good correlation between minimal 2D and 3D diameters and underestimation of maximal VSD diameter by 2D. Cheng *et al.*¹⁰ also found that defect sizes obtained by 3D TTE had better correlation with surgical findings than those obtained by 2D TTE.

A new understanding of measurement differences between the two imaging methods, and according to VSD location, was offered by analysis of VSD shape using 3D TTE. VSD morphology could be

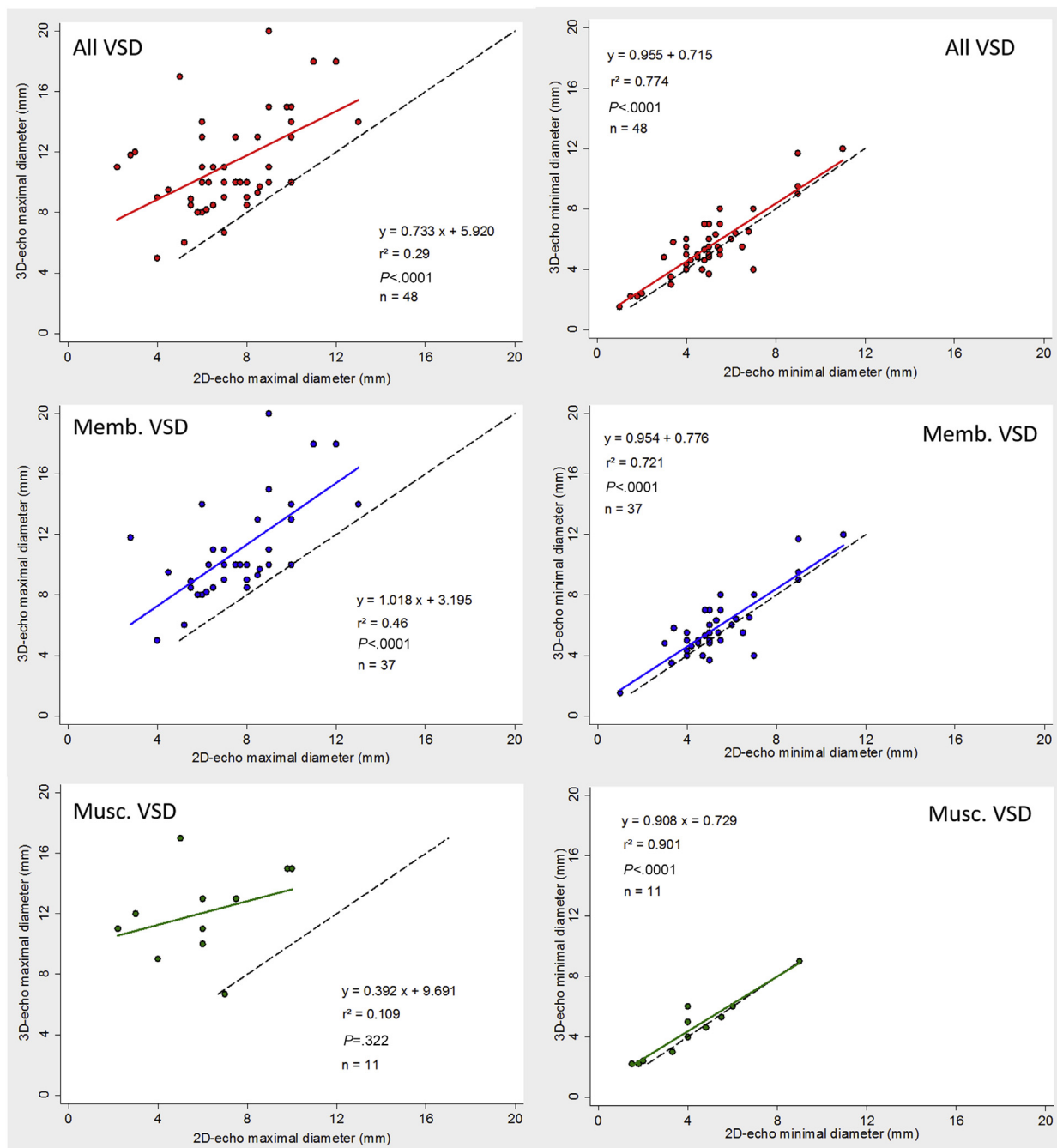


Figure 2 Linear regression analysis plotting VSD diameters estimated by 3D versus 2D TTE in the whole population and in subgroups according to VSD position. *Dashed lines* represent lines of identity, and *solid lines* represent linear regression.

depicted in all cases. VSDs were oval rather than round in shape, as assessed quantitatively by maximal-to-minimal diameter ratio. The minimal diameter was always in the long-axis orientation, while the maximal diameter was in elevation orientation. The maximal-to-minimal diameter ratio was underestimated by 2D TTE compared with 3D TTE because of maximal VSD diameter discrepancies. The maximal-to-minimal diameter ratio was more pronounced and highly variable in muscular VSDs. VSD shape can be very different, ranging from oval or crescent-shaped to slit-shaped defects.

Moreover, VSD measurements vary significantly during the cardiac cycle. Real-time 3D en face views offer a direct visualization of VSD shape motion from either the left or right ventricle. We quantified measurement variation using 3D TTE. The mean variation of VSD surface area during the cardiac cycle was $32 \pm 15\%$, less than previously described by our team for atrial septal defects ($68 \pm 15\%$). Area variation was greater in muscular defects than in membranous defects. Muscular defects are surrounded in their entire circumference by muscular contractile tissues, while membranous defects are bordered at their upper parts by fibrous aortic

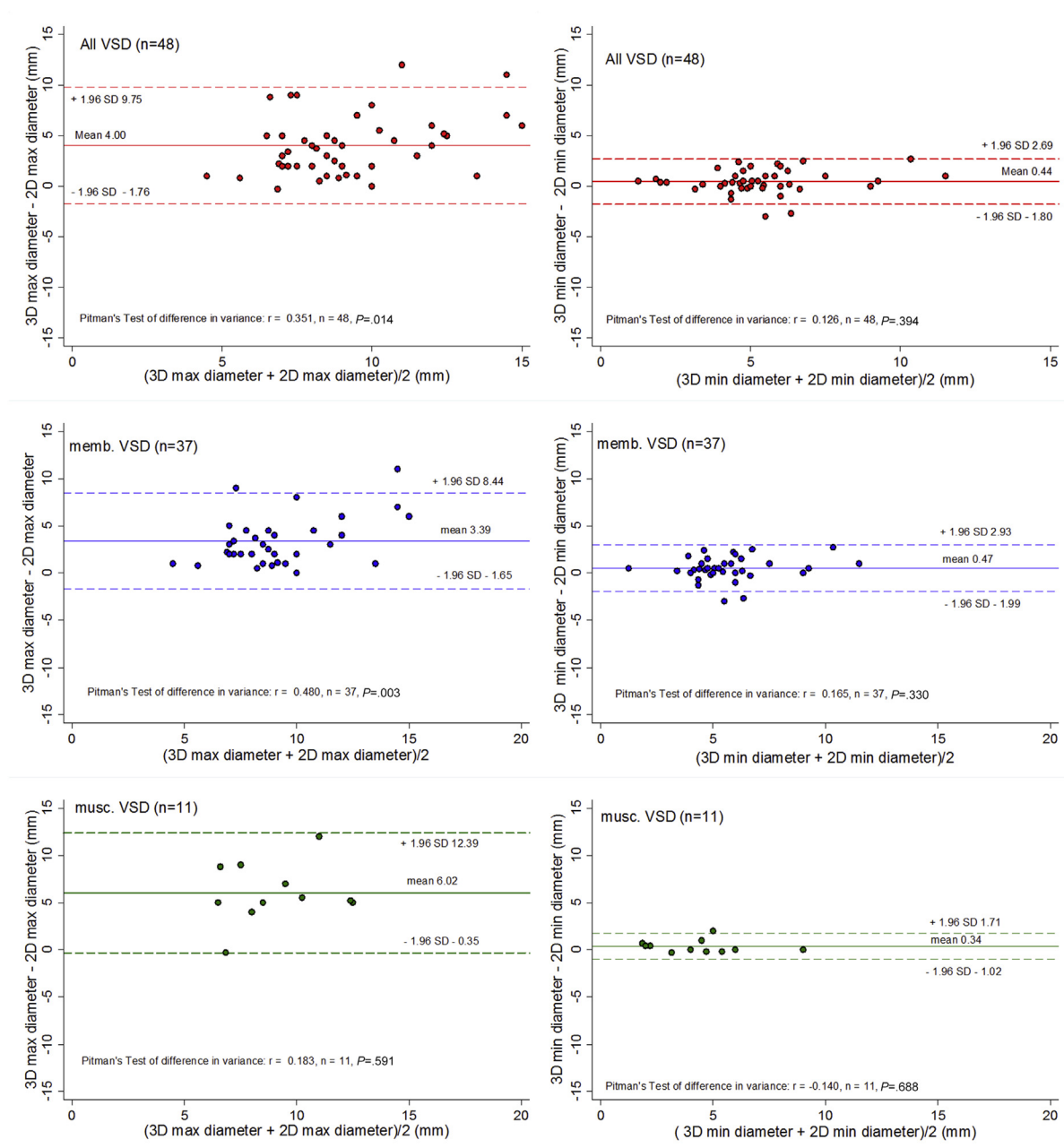


Figure 3 Bland-Altman graphs comparing VSD diameters obtained by 2D and 3D TTE in the whole population and in subgroups according to VSD position. *Solid lines* represent average differences, and *dashed lines* represent 95% limits of agreement.

Table 3 VSD maximal diameters by 2D TTE, 3D TTE, and surgery in patients with surgical VSD closure

	2D TTE (n = 15)	3D TTE (n = 15)	Surgical (n = 15)	P		
Maximal VSD diameter (mm)	8.5 ± 2.3	11.9 ± 3.4	12.2 ± 3.4	2D TTE vs 3D TTE <.0001	2D TTE vs surgery <.001	3D TTE vs surgery .07

Data are expressed as mean ± SD. P values by Wilcoxon signed rank test.

annular tissues, which are not contractile. This observation may have an impact on shunt severity assessment. Shunting across a VSD occurs mainly during systole, and VSD measurements may be interesting in this cardiac phase.

Recently introduced catheter-based techniques for device closure of VSDs require accurate measurements of the defects to choose the appropriate device, increase the success rate, and reduce complications.^{6,21,22} Some of these complications

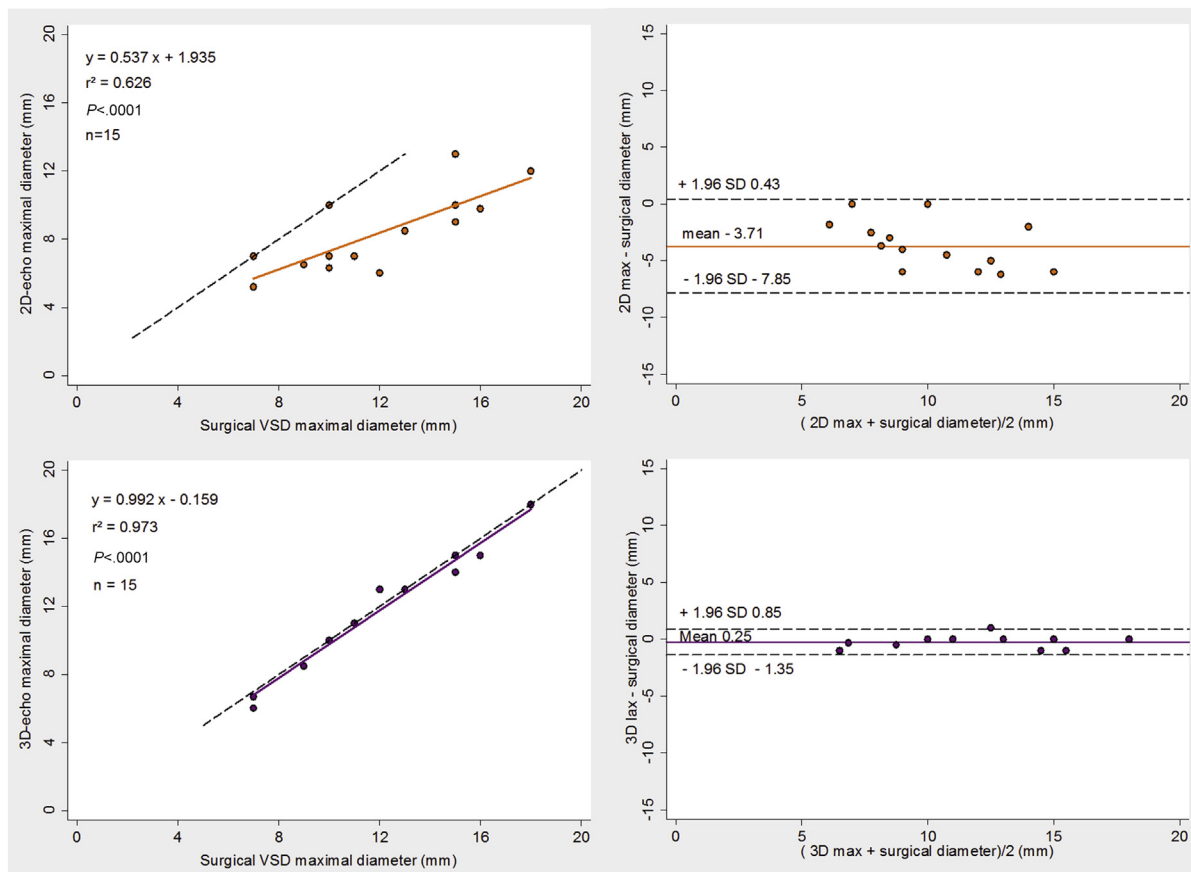


Figure 4 Linear regression analysis plotting VSD diameters estimated by 3D and 2D TTE versus surgical findings. *Dashed lines* represent lines of identity, and *solid lines* represent linear regression. Bland-Altman graphs comparing VSD diameters obtained by 2D and 3D TTE compared with surgical findings. *Solid lines* represent average differences, and *dashed lines* represent 95% limits of agreement.

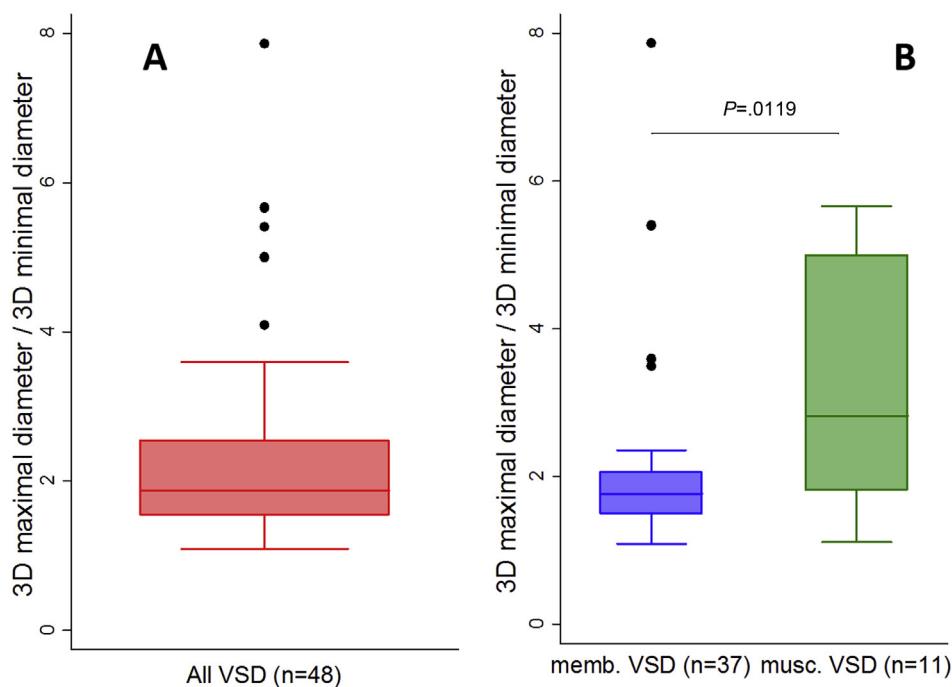


Figure 5 Box-plot graphs of VSD asymmetry ratio estimated by 3D TTE in the whole population (**A**) and in subgroups according to defect position (**B**).

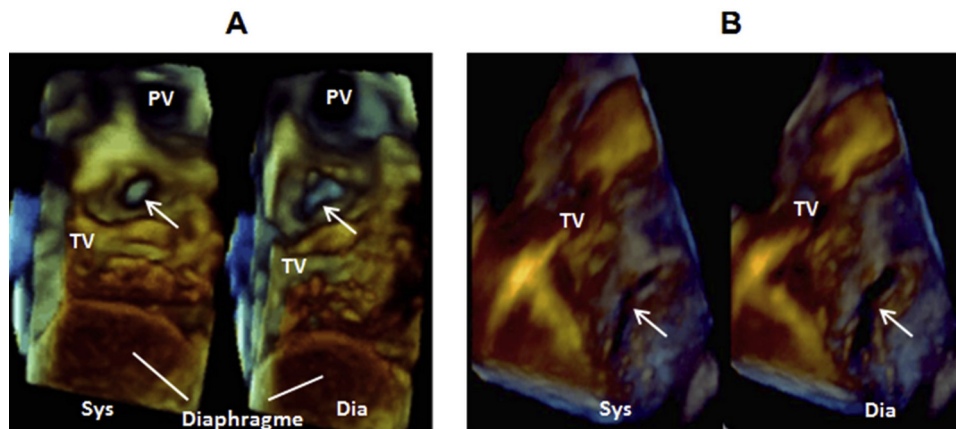


Figure 6 Right ventricular 3D transthoracic echocardiographic en face view of a membranous (**A**) and a muscular (**B**) VSD surface area (arrows) displaying variation of morphology during the cardiac cycle. *Dia*, Diastole; *PV*, pulmonary valve; *Sys*, systole; *TV*, tricuspid valve.

may be related to underestimation of defect size by 2D echocardiography⁵; others may have been caused by the use of an oversized device. Several devices of variable configuration are available actually for the percutaneous closure of VSDs.^{3,4,23} Three-dimensional echocardiography could be useful in the selection of the appropriate occlusion device configuration according to VSD morphology.²⁴ However, in this study we did not evaluate this potential application, and further studies are needed to determine the value of this approach.

Study Limitations

The main limitation of our study was the small size of the surgical group. Surgical sizing is considered the gold standard. However, only children with pulmonary arterial hypertension and/or heart failure symptoms were treated surgically at the time of study. Despite the small number, there was a close correspondence with 3D transthoracic echocardiographic measurements (statistically significant).

CONCLUSIONS

Three-dimensional echocardiography is useful to assess measurements and shapes of VSDs in children. It allows better VSD morphologic and maximal diameter assessment compared with 2D echocardiography. Irregularity of VSD shape and its changes during the cardiac cycle can be visually and quantitatively displayed. Three-dimensional echocardiography may be particularly useful before and during percutaneous closure of VSDs.

SUPPLEMENTARY DATA

Supplementary data related to this article can be found at <http://dx.doi.org/10.1016/j.echo.2016.04.012>.

REFERENCES

1. Penny DJ, Vick GW 3rd. Ventricular septal defect. *Lancet* 2011;377:1103-12.
2. Vargas Barron J, Sahn DJ, Valdes-Cruz LM, Lima CO, Goldberg SJ, Grenadier E, et al. Clinical utility of two-dimensional Doppler echocardiographic techniques for estimating pulmonary to systemic blood flow ratios in children with left to right shunting atrial septal defect, ventricular septal defect or patent ductus arteriosus. *J Am Coll Cardiol* 1984;3:169-78.
3. Chungsomprasong P, Durongpisitkul K, Vijarnsorn C, Soongswang J, Le TP. The results of transcatheter closure of VSD using Amplatzer(R) device and Nit Occlud(R) Le coil. *Catheter Cardiovasc Interv* 2011;78:1032-40.
4. Chen F, Li P, Liu S, Du H, Zhang B, Jin X, et al. Transcatheter closure of intracristal ventricular septal defect with mild aortic cusp prolapse using zero eccentricity ventricular septal defect occluder. *Circ J* 2015;79:2162-8.
5. Holzer R, Balzer D, Cao QL, Lock K, Hijazi ZM, Amplatzer Muscular Ventricular Septal Defect Investigators. Device closure of muscular ventricular septal defects using the Amplatzer muscular ventricular septal defect occluder: immediate and mid-term results of a U.S. registry. *J Am Coll Cardiol* 2004;43:1257-63.
6. Fu YC. Transcatheter device closure of muscular ventricular septal defect. *Pediatr Neonatol* 2011;52:3-4.
7. Hsu JH, Wu JR, Dai ZK, Lee MH. Real-time three-dimensional echocardiography provides novel and useful anatomic insights of perimembranous ventricular septal aneurysm. *Int J Cardiol* 2007;118:326-31.
8. Mercer-Rosa L, Seliem MA, Fedec A, Rome J, Rychik J, Gaynor JW. Illustration of the additional value of real-time 3-dimensional echocardiography to conventional transthoracic and transesophageal 2-dimensional echocardiography in imaging muscular ventricular septal defects: does this have any impact on individual patient treatment? *J Am Soc Echocardiogr* 2006;19:1511-9.
9. Mehmood F, Miller AP, Nanda NC, Patel V, Singh A, Duncan K, et al. Usefulness of live/real time three-dimensional transthoracic echocardiography in the characterization of ventricular septal defects in adults. *Echocardiography* 2006;23:421-7.
10. Cheng TO, Xie MX, Wang XF, Wang Y, Lu Q. Real-time 3-dimensional echocardiography in assessing atrial and ventricular septal defects: an echocardiographic-surgical correlative study. *Am Heart J* 2004;148:1091-5.
11. Acar P, Saliba Z, Bonhoeffer P, Aggoun Y, Bonnet D, Sidi D, et al. Influence of atrial septal defect anatomy in patient selection and assessment of

- closure with the Cardioseal device; a three-dimensional transoesophageal echocardiographic reconstruction. *Eur Heart J* 2000;21:573-81.
12. Hascoet S, Hadeed K, Marchal P, Dulac Y, Alacoque X, Heitz F, et al. The relation between atrial septal defect shape, diameter, and area using three-dimensional transoesophageal echocardiography and balloon sizing during percutaneous closure in children. *Eur Heart J Cardiovasc Imaging* 2015;16:747-55.
 13. Bland JM, Altman DG. Statistical methods for assessing agreement between two methods of clinical measurement. *Lancet* 1986;1:307-10.
 14. van den Heuvel F, Timmers T, Hess J. Morphological, haemodynamic, and clinical variables as predictors for management of isolated ventricular septal defect. *Br Heart J* 1995;73:49-52.
 15. Cossor W, Cui VW, Roberson DA. Three-dimensional echocardiographic en face views of ventricular septal defects: feasibility, accuracy, imaging protocols and reference image collection. *J Am Soc Echocardiogr* 2015;28:1020-9.
 16. Dall'Agata A, Cromme-Dijkhuis AH, Meijboom FJ, McGhie JS, Bol-Raap G, Nosir YF, et al. Three-dimensional echocardiography enhances the assessment of ventricular septal defect. *Am J Cardiol* 1999;83:1576-9. A8.
 17. Kardon RE, Cao QL, Masani N, Sugeng L, Supran S, Warner KG, et al. New insights and observations in three-dimensional echocardiographic visualization of ventricular septal defects: experimental and clinical studies. *Circulation* 1998;98:1307-14.
 18. Acar P, Abdel-Massih T, Douste-Blazy MY, Dulac Y, Bonhoeffer P, Sidi D. Assessment of muscular ventricular septal defect closure by transcatheter or surgical approach: a three-dimensional echocardiographic study. *Eur J Echocardiogr* 2002;3:185-91.
 19. Chen FL, Hsiung MC, Nanda N, Hsieh KS, Chou MC. Real time three-dimensional echocardiography in assessing ventricular septal defects: an echocardiographic-surgical correlative study. *Echocardiography* 2006;23:562-8.
 20. van den Bosch AE, Ten Harkel DJ, McGhie JS, Roos-Hesselink JW, Simoons ML, Bogers AJ, et al. Feasibility and accuracy of real-time 3-dimensional echocardiographic assessment of ventricular septal defects. *J Am Soc Echocardiogr* 2006;19:7-13.
 21. Acar P, Abadir S, Aggoun Y. Transcatheter closure of perimembranous ventricular septal defects with Amplatzer occluder assessed by real-time three-dimensional echocardiography. *Eur J Echocardiogr* 2007;8:110-5.
 22. Knauth AL, Lock JE, Perry SB, McElhinney DB, Gauvreau K, Landzberg MJ, et al. Transcatheter device closure of congenital and postoperative residual ventricular septal defects. *Circulation* 2004;110:501-7.
 23. Kanaan M, Ewert P, Berger F, Assa S, Schubert S. Follow-up of patients with interventional closure of ventricular septal defects with Amplatzer Duct Occluder II. *Pediatr Cardiol* 2015;36:379-85.
 24. Charakida M, Qureshi S, Simpson JM. 3D echocardiography for planning and guidance of interventional closure of VSD. *JACC Cardiovasc Imaging* 2013;6:120-3.

Video 1 Multiplanar reconstruction analysis of a membranous VSD.

Video 2 Right ventricular 3D transthoracic echocardiographic en face view of a membranous VSD, displaying its morphologic variation during the cardiac cycle.

Video 3 Right ventricular 3D transthoracic echocardiographic en face view of a muscular VSD, displaying its morphologic variation during the cardiac cycle.